Iranian Journal of Basic Medical Sciences
ijbms.mums.ac.ir

Cannabidiol attenuates lung ischemia-reperfusion injury by modulating RIPK1/RIPK3-mediated necroptosis and HIF-1α/VEGF signaling

Hasan Ekrem Camas [1]*, Mehtap Savran [2], Serap Yildirim [1], Suleyman Emre Akin [1], Rasih Yazkan [1], Ilter Ilhan [3], Muhammet Yusuf Tepebasi [4], Mehmet Abdulkadir Sevuk [2], Ozlem Ozmen [5]

[1] Department of Thoracic Surgery, Faculty of Medicine, Suleyman Demirel University, Isparta, Türkiye
[2] Department of Pharmacology, Faculty of Medicine, Suleyman Demirel University, Isparta 32200, Türkiye
[3] Department of Biochemistry, Faculty of Medicine, Suleyman Demirel University, Isparta 32200, Türkiye
[4] Department of Genetic, Faculty of Medicine, Suleyman Demirel University, Isparta 32200, Türkiye
[5] Department of Pathology, Faculty of Veterinary, Burdur Mehmet Akif Ersoy University, Burdur 15000, Türkiye

ARTICLE INFO

Article type:
Original

Article history:
Received: Jul 29, 2025
Accepted: Mar 8, 2026

Keywords:
Cannabidiol
Hypoxia-Inducible factor 1 - alpha subunit
Ischemia
Lung injury
Necroptosis
Oxidative stress
Reperfusion
Vascular endothelial growth - factor A

ABSTRACT

Objective(s): Lung ischemia-reperfusion (IR) injury is a critical clinical condition characterized by oxidative stress, inflammation, and necroptosis, often leading to severe complications. Cannabidiol (CBD), a non-psychoactive cannabinoid, has demonstrated anti-oxidant and anti-inflammatory properties, but its role in modulating lung IR injury remains incompletely understood. This study investigated the protective effects of CBD on lung IR injury in rats, focusing on the RIPK1/RIPK3 necroptosis pathway and the HIF-1α/VEGF/eNOS signaling axis.

Materials and Methods: Forty male Wistar albino rats were randomized into four groups: control, IR, IR+CBD (5 mg/kg), and CBD-only. Histopathological, immunohistochemical (TNF-α, Caspase-3), biochemical (TOS, TAS, OSI), and gene expression (RIPK1, RIPK3, HIF-1α, VEGF, eNOS) analyses were performed. The IR group exhibited significant oxidative stress, inflammation, and tissue damage, with elevated TNF-α, caspase-3, TOS, OSI, and necroptosis/apoptosis markers.

Results: CBD treatment markedly attenuated these effects, reducing oxidative stress (↑TAS, ↓TOS/OSI), suppressing inflammation (↓TNF-α), and inhibiting both apoptotic (↓Caspase-3) and necroptotic (↓RIPK1/RIPK3) pathways. Additionally, CBD down-regulated HIF-1α/VEGF/eNOS expression, suggesting modulation of hypoxia-responsive signaling.

Conclusion: These findings demonstrate that CBD mitigates lung IR injury by targeting oxidative stress, inflammation, and cell death mechanisms, highlighting its potential as a therapeutic agent. Further preclinical and clinical studies are warranted to validate these results.

▶Please cite this article as:
Camas HE, Savran M, Yildirim S, Akin SE, Yazkan R, Ilhan I, Tepebasi MY, Sevuk MA, Ozmen O. Cannabidiol attenuates lung ischemia-reperfusion injury by modulating RIPK1/RIPK3-mediated necroptosis and HIF-1α/VEGF signaling. Iran J Basic Med Sci 2026; 29: 766-773. doi: https://dx.doi.org/10.22038/ijbms.2026.90024.19406

Introduction

Ischemic damage refers to insufficient blood flow to tissues or organs, while reperfusion refers to the restoration of blood flow after ischemia (1). The cellular damage caused by these processes is known as ischemia-reperfusion (IR) damage (2). In the lungs, IR damage frequently occurs during procedures such as cardiopulmonary bypass, pulmonary thromboendarterectomy, and lung transplantation. It can also develop in other parts of the body due to distant organ ischemia (2, 3).

Oxidative stress arises when the delicate equilibrium between pro-oxidant species and the anti-oxidant defense system is disrupted (4). This imbalance is triggered by increased levels of reactive oxygen species (ROS) following IR, which in turn stimulates oxidative stress and inflammatory responses (5, 6). ROS, interleukin-6, and tumor necrosis factor-alpha (TNF-α) are major cytokines in tissue damage during IR (7).

The transcription factor hypoxia-inducible factor-1 alpha (HIF-1α), which regulates angiogenesis, erythropoiesis, energy metabolism, and cell survival, is functionally activated in hypoxic environments (8, 9). Upon activation, HIF-1α suppresses the tumor suppressor protein p53 and promotes the expression of angiogenic factors, including vascular endothelial growth factor (VEGF) and endothelial nitric oxide synthase (eNOS), thereby protecting cells from hypoxic injury (6, 10). VEGF, in particular, plays a crucial role in stimulating the growth, proliferation, and differentiation of vascular endothelial cells and in maintaining vascular permeability (11).

Within the spectrum of regulated cell death modalities, apoptosis and necroptosis have emerged as focal points of

*Corresponding author: Hasan Ekrem Camas. Department of Thoracic Surgery, Suleyman Demirel University Research and Education Hospital , 257th Street, Çünür, Doğu yerleşkesi, 32260, Isparta, Türkiye. Tel: +90 2462119255, Email: hasancamas@sdu.edu.tr

intensive scientific inquiry (12). Apoptosis proceeds via intrinsic and extrinsic pathways, both of which involve caspase activation (13, 14). In the extrinsic pathway, death ligands such as FasL and TNF-α bind to death receptors such as Fas and TNFR, initiating the death-inducing signal complex (DISC) and activating caspase-8 (13-15). Caspase-8, in turn, activates caspase-3 (Cas-3), a central player in the apoptosis pathway (13-15). In the intrinsic pathway, the release of mitochondrial cytochrome c, resulting from the inactivation of Bcl proteins, triggers caspase-8 activation and leads to cell death (16). Necroptosis is a form of regulated cell death that operates through a well-defined signaling cascade involving the receptor-interacting serine/threonine-protein kinases RIPK1 and RIPK3, as well as the pseudokinase mixed lineage kinase domain-like protein (MLKL). This programmed necrotic pathway is distinct from apoptosis and is typically activated under conditions where apoptotic signaling is impaired or inhibited (17, 18). TNF-α plays a pivotal role in promoting necroptosis by up-regulating the expression of RIPK1 and RIPK3, thereby facilitating the formation of the necrosome complex and the downstream activation of MLKL. In addition to contributing to inflammatory responses, the activation of this pathway has been connected to other clinical conditions, including tissue damage and inflammatory disorders (19, 20).

Cannabidiol (CBD), a phytocannabinoid isolated from *Cannabis sativa*, displays a broad pharmacological profile—most notably anti-inflammatory and antinecrotic activities—positioning it as a promising therapeutic candidate for ameliorating ischemic tissue injury (21-23). Owing to its comparatively weak binding affinity for CB1 and CB2 cannabinoid receptors, CBD functions as a functional antagonist that modulates downstream inflammatory signalling pathways (24). Its anti-oxidant effect stems from its ability to reduce ROS production and inhibit TNF-α release (25). This study aims to investigate how CBD alleviates lung IR injury via RIPK1/RIPK3-mediated necroptosis and HIF-1α/VEGF/eNOS pathway.

Materials and Methods

Ethics and experimental design

The Suleyman Demirel University Committee on Animal Research gave its approval to all experimental procedures, following the guidelines of the National Institutes of Health for animal research (Approval No. 26.01.23-01/119). The study received funding from the Scientific Research Fund of Suleyman Demirel University (Project No. TSG-2023-9010).

Forty male Wistar Albino rats weighing between 300 and 350 grams were utilized in the experiment. Rats were housed in controlled environments (temperature: 21–22 °C, 12-hr light and dark cycle) and were given unrestricted access to water and food. They were kept in Euro-type 4 cages. Four experimental groups were randomly selected from among the rats, each consisting of 10 rats, as described below:

Group I (Control) (n=10): Rats received intraperitoneal (IP) injections of 1 ml of saline. A thoracotomy was performed without inducing IR. The hilum of the lung was visualized.

Group II (IR) (n=10): Rats received IP injections of 1 ml of saline. Following a left thoracotomy, ischemia was induced by completely clamping the hilum for 60 min, and then reperfusion was performed for another 60 min (26, 27)

Group III (IR-CBD) (n=10): Rats received injections of 5 mg/kg CBD IP Following a left thoracotomy, ischemia was induced by completely clamping the hilum for 60 min, and then reperfusion was performed for another 60 min (27).

Group IV (CBD) (n=10): Rats received injections of 5 mg/kg CBD IP A thoracotomy was performed, but IR was not induced (28, 29).

Prior to anesthesia, all animals were fasted for 12 hr. Anesthesia was induced by administering xylazine (10 mg/kg; Xylazinbio, Bioveta, Czech Republic) and ketamine (90 mg/kg; Keta-Kontrol, Doğa Drug, Türkiye) IP. Following thoracotomy and shaving of the thoracic region, a non-traumatic vascular clamp was applied to the left lung hilum for 60 min in the IR and IR-CBD groups, followed by reperfusion for 60 min. After confirming successful reperfusion, the rats were sacrificed with the surgical exsanguination method. Lung and blood samples were collected for biochemical, immunohistochemical, and mRNA analyses. Tissues for histopathology were fixed in formaldehyde, while those for biochemical and mRNA analyses were preserved at appropriate temperatures.

Histopathological examination

At the end of the study, all animals were euthanised under deep anaesthesia, the lungs were excised, and specimens were immediately fixed in 10 % neutral-buffered formalin. A 48-hr fixation phase was followed by tissue processing in an automated tissue processor and paraffin wax embedding. Serial 5 µm sections were obtained with a rotary microtome, mounted on glass slides, stained with haematoxylin–eosin, and examined by light microscopy for histopathological appraisal. Histopathological alterations, including hyperemia, edema, inflammatory cell infiltration, and epithelial cell loss, were scored semi-quantitatively on a scale from 0 to 3 according to the criteria described by Ozmen *et al.* 2024 (30) (Table 1). Morphometric assessments and photomicrograph documentation were carried out using the Cell Sens Life Science Imaging Software System

Table 1. Histopathological scoring criteria for lung tissue

Score	Hyperemia	Edema	Infiltrations	Epithelial loss
0	Normal thin alveolar septae	No edema	Less than 5 in the fields	None
1	Slight hyperemic alveolar septae (in less than 1/3 of the fields)	Slight edema (in less than 1/3 of the fields)	5 to 10 in the fields	Slight loss (in less than 1/3 of the fields)
2	Moderate hyperemic alveolar septae (in 1/3 to 2/3 of the fields)	Moderate edema (in 1/3 to 2/3 of the fields)	10 to 20 in the fields	Moderate loss (in 1/3 to 2/3 of the fields)
3	Severe hyperemic alveolar septae (in greater than 2/3 of the fields)	Severe edema (in greater than 2/3 of the fields)	More than 20 in the fields	Severe loss (in greater than 2/3 of the fields)

Examinations were done high-power field (HPF) (10 fields of view at ×400 magnification).

Table 2. Primary Sequences, Product Sizes, and Accession Numbers of Genes in Experimental Animals

Genes	Primary sequence	Product size	Accession number
GAPDH (Housekeeping)	F: AGTGCCAGCCTCGTCTCATA	248 bp	NM_017008.4
	R: GATGGTGATGGGTTTCCCGT		
VEGF	F: TTCGTCCAACTTCTGGGCTC	482 bp	NM_001287111.1
	R: GCTTTCTGCTCCCCTTCTGT		
RIPK1	F: ACCTTAGACGCGTAGGAGCG	527 bp	NM_001107350.1
	R: TCATTGTACTCAGCGCGGTT		
RIPK3	F: TAGTTTATGAAATGCTGGACCGC	145 bp	NM_139342.2
	R: GCCAAGGTGTCAGATGATGTCC		
HIF-1α	GCAACTAGGAACCCGAACCA	251 bp	NM_024359.2
	TCGACGTTCGGAACTCATCC		
eNOS	F: GGTTGACCAAGGCAAACCAC	247 bp	NM_021838.2
	R: CCTAATACCACAGCCGGAGG		

F: Forward, R: Reverse, GAPDH: Glyceraldehyde-3-phosphate dehydrogenase; VEGF: Vascular endothelial growth factor; RIPK1: Receptor-interacting serine-threonine kinase 1; RIPK3: Receptor-interacting serine-threonine kinase 3; eNOS: Endothelial nitric oxide synthase; HIF-1α: Hypoxia-inducible factor 1 alpha

(Olympus Co., Tokyo, Japan). The resulting data were then analyzed statistically.

Immunohistochemical examination

Two sections from each paraffin block were put on poly-L-lysine-coated slides and immunohistochemically stained for TNF-α and Cas-3 using the streptavidin-biotin method in accordance with the manufacturer's instructions. Primary antibodies used included anti-TNF (sc-52746, 1/100) and anti-Cas-3 (sc-7272). Following overnight primary-antibody incubation, antigen detection was completed by sequentially applying a biotinylated secondary antibody and a streptavidin–alkaline phosphatase complex, in accordance with the manufacturer's protocol for the Mouse and Rabbit Specific HRP/AEC Detection IHC Kit (Abcam, ab93705). Aminoethyl carbazole was employed as the chromogenic substrate. For negative controls, primary antibodies were replaced with antigen dilution solution. The samples were blindly analyzed by a certified pathologist, and the percentage of immunostained cells in ten fields per rat was calculated at 40x magnification using ImageJ software (NIH, version 1.48). Positive staining was identified by a strong red color, and the Olympus Database Manual Cell Sens System was used to take pictures.

Biochemical analysis

As part of the biochemical evaluation, total anti-oxidant status (TAS) and total oxidant status (TOS) were quantified, and the oxidative stress index (OSI) was subsequently computed. Pulmonary tissue samples were homogenised in a phosphate buffer maintained at pH 7.4. To get rid of cell debris, the homogenates were centrifuged for 10 min at 10,000 × g. A Beckman Coulter AU5800 (Beckman Coulter, USA) and kits from Rel Assay Diagnostics (Gaziantep, Türkiye) were used to measure TAS and TOS spectrophotometrically. The formula used to calculate the OSI was OSI=(TOS / TAS) x 100 (31).

mRNA analysis

Reverse transcription–polymerase chain reaction (RT-qPCR)

Total RNA was extracted from homogenised tissue using the GeneAll RiboEx™ RNA Isolation Kit (GeneAll Biotechnology, Seoul, South Korea) by the manufacturer's protocol. RNA concentration and purity were assessed with a BioSpec-nano spectrophotometer (Shimadzu Corporation, Kyoto, Japan). Thereafter, 1 µg of RNA was reverse-transcribed to complementary DNA employing the A.B.T.™ cDNA Synthesis Kit (Atlas Biotechnology, Türkiye) on a thermal cycler.

The NCBI database was used to generate primers for particular mRNA sequences (Table 2). GAPDH was employed as the housekeeping gene in the analysis of gene expression utilizing a Bio-Rad CFX96 RT-PCR and 2X SYBR Green master mix (Nepenthe, Türkiye). Every sample was analyzed in triplicate, and the reaction volume was set at 20 µL. The kit's instructions for thermal cycling were followed. Relative mRNA expression was quantified and normalised via the comparative $2^{-\Delta\Delta Ct}$ algorithm.

Statistical analysis

Statistical analyses were performed with SPSS software, version 22.0. Normality was verified with the Shapiro–Wilk test. Because the data conformed to a Gaussian distribution (P>0.05), inter-group differences were assessed by one-way analysis of variance (ANOVA), and pairwise contrasts were resolved using Tukey's post-hoc test, with statistical significance set at P<0.05. Variables deviating from normality were analysed with the Mann–Whitney U test, and multiple non-parametric comparisons were adjusted by Dunnett's C procedure. Histopathological score data were analyzed using the Kruskal–Wallis test and are presented as median ± interquartile range (IQR).

Results

Histopathological findings

Microscopic examination of the lung tissues from the control and CBD groups revealed normal lung histoarchitecture. In the IR group, edema, pronounced hyperemia, epithelial loss, and inflammation were observed (P<0.001). However, in the IR-CBD group, CBD treatment notably alleviated these pathological alterations (P<0.001) (Figure 1).

Immunohistochemical findings

Immunohistochemical analysis of the control group revealed minimal or almost undetectable expression levels of Cas-3 and TNF-α. In contrast, the IR group showed significant up-regulation of both markers (P<0.001). The

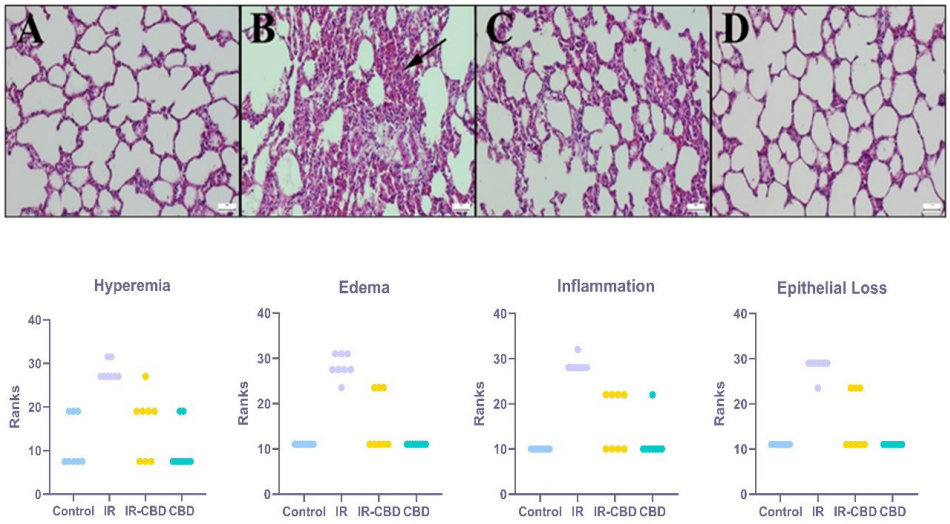

Figure 1. Histopathological assessment of rat lung tissues across the experimental groups revealed the following
(A) normal lung histology was observed in the control group; (B) the IR group presented increased septal tissue thickness and significant hemorrhage (denoted by arrows); (C) the IR-CBD group presented a reduction in pathological findings; (D) normal tissue architecture was noted in the CBD group. HE staining was employed, with scale bars set at 50 µm. The values are reported as median ± IQR. Statistical significance is defined as **P*<0.05, ***P*<0.01, and ****P*<0.001. CBD: Cannabidiol; HE: Hematoxylin–eosin; IR: Ischemia/reperfusion

IR-CBD group exhibited a significant reduction in TNF-α and Cas-3 expression compared to the IR group (*P*<0.001). Additionally, compared to the injury group, the CBD-only group demonstrated significant reductions in both TNF-α and Cas-3 levels, highlighting the effectiveness of CBD in mitigating these markers (*P*<0.001 for both). Notably, Cas-3 expression was significantly higher in the IR-CBD group than in both the control and CBD groups (*P*<0.01). The primary localization of these proteins was in inflammatory cells, alveolar macrophages, and alveolar epithelial cells, as shown in Figure 2.

Biochemical analyses results

Biochemical analysis revealed significantly higher levels of TOS and OSI and lower levels of TAS in the IR group compared to the control group (*P*<0.001 for all comparisons). After CBD treatment, OSI levels decreased significantly (*P*<0.001), and TAS levels increased (*P*<0.001). In comparison with the IR group, the CBD group displayed significantly lower TOS and OSI levels and higher TAS levels

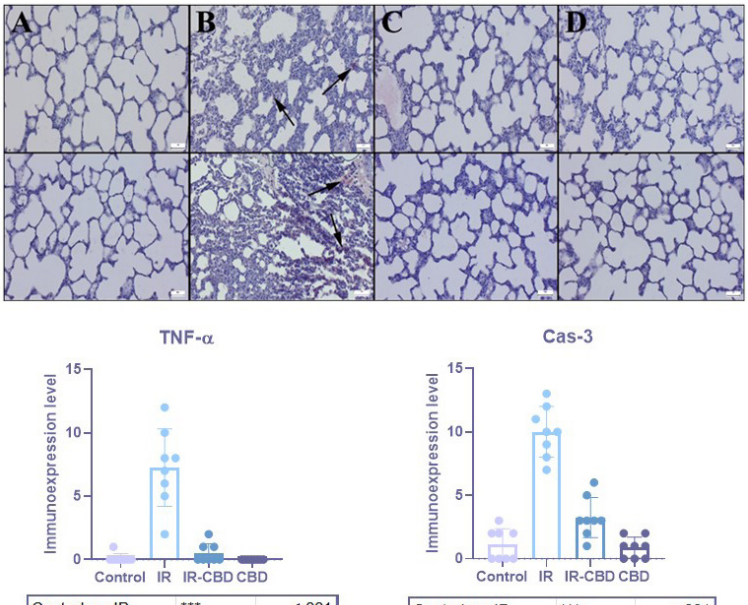

Control vs. IR	***	<.001
Control vs. IR-CBD	ns	0.64
Control vs. CBD	ns	0.876
IR vs. IR-CBD	***	<.001
IR vs. CBD	***	<.001
IR-CBD vs. CBD	ns	0.533

Control vs. IR	***	<.001
Control vs. IR-CBD	**	0.008
Control vs. CBD	ns	0.738
IR vs. IR-CBD	***	<.001
IR vs. CBD	***	<.001
IR-CBD vs. CBD	**	0.003

Figure 2. Immunoexpression of Caspase-3 (Cas-3) is shown in the upper row, and that of tumor necrosis factor-alpha (TNF-α) is shown in the lower row across the studied rat groups
Staining was performed via the streptavidin–biotin peroxidase method, with scale bars set at 50 µm. Cas-3: Caspase-3; TNF-α: Tumor necrosis factor-alpha; IR: Ischemia/reperfusion; CBD: Cannabidiol. The data are presented as the means ± standard deviations (SDs). Statistical significance is marked as **P*<0.05, ***P*<0.01, and ****P*<0.001.

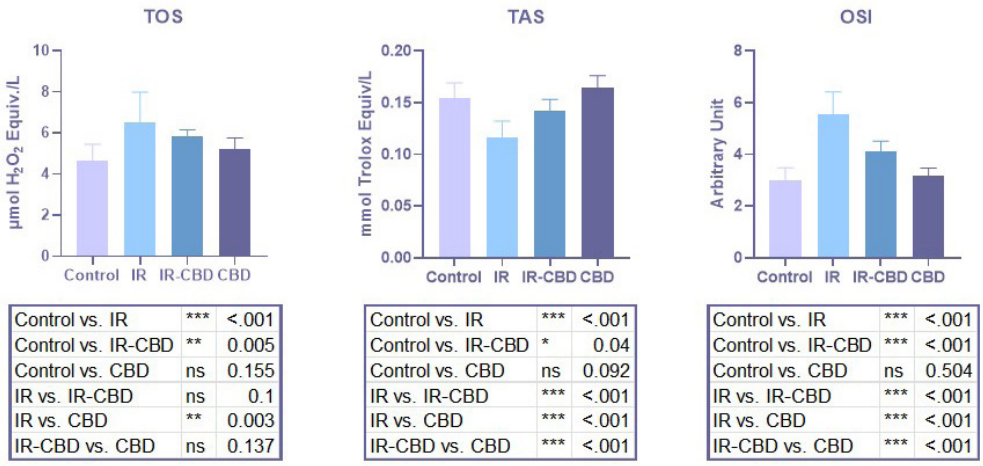

Control vs. IR	***	<.001
Control vs. IR-CBD	**	0.005
Control vs. CBD	ns	0.155
IR vs. IR-CBD	ns	0.1
IR vs. CBD	**	0.003
IR-CBD vs. CBD	ns	0.137

Control vs. IR	***	<.001
Control vs. IR-CBD	*	0.04
Control vs. CBD	ns	0.092
IR vs. IR-CBD	***	<.001
IR vs. CBD	***	<.001
IR-CBD vs. CBD	***	<.001

Control vs. IR	***	<.001
Control vs. IR-CBD	***	<.001
Control vs. CBD	ns	0.504
IR vs. IR-CBD	***	<.001
IR vs. CBD	***	<.001
IR-CBD vs. CBD	***	<.001

Figure 3. Oxidative stress parameters in rat lungs
IR represents ischemia/reperfusion, CBD denotes cannabidiol, TOS stands for total oxidant status, TAS refers to total antioxidant status, and OSI indicates the oxidative stress index. The values are reported as the means ± standard deviations (SDs). Statistical significance is defined as **P*<0.05, ***P*<0.01, and ****P*<0.001. CBD: Cannabidiol; HE: Hematoxylin–eosin; IR: Ischemia/reperfusion; TAS: Total antioxidant status; OSI: Oxidative stress index; TOS: Total oxidant status

(*P*<0.01, *P*<0.001, and *P*<0.001, respectively). Moreover, the TAS levels in the CBD group were significantly greater than those in the IR-CBD group (*P*<0.001), and OSI levels were significantly lower in the CBD group compared to the IR-CBD group (*P*<0.001) (Figure 3).

mRNA analyses results

In comparison to the control group, the IR group's relative mRNA expression levels demonstrated a substantial rise in each of the five metrics (*P*<0.001 for each). In contrast, the IR-CBD group demonstrated a significant decrease in all parameters relative to the IR group (*P*<0.001 for all comparisons). Furthermore, the CBD group exhibited significantly lower levels of all markers compared to the IR group (*P*<0.001 for each) (Figure 4).

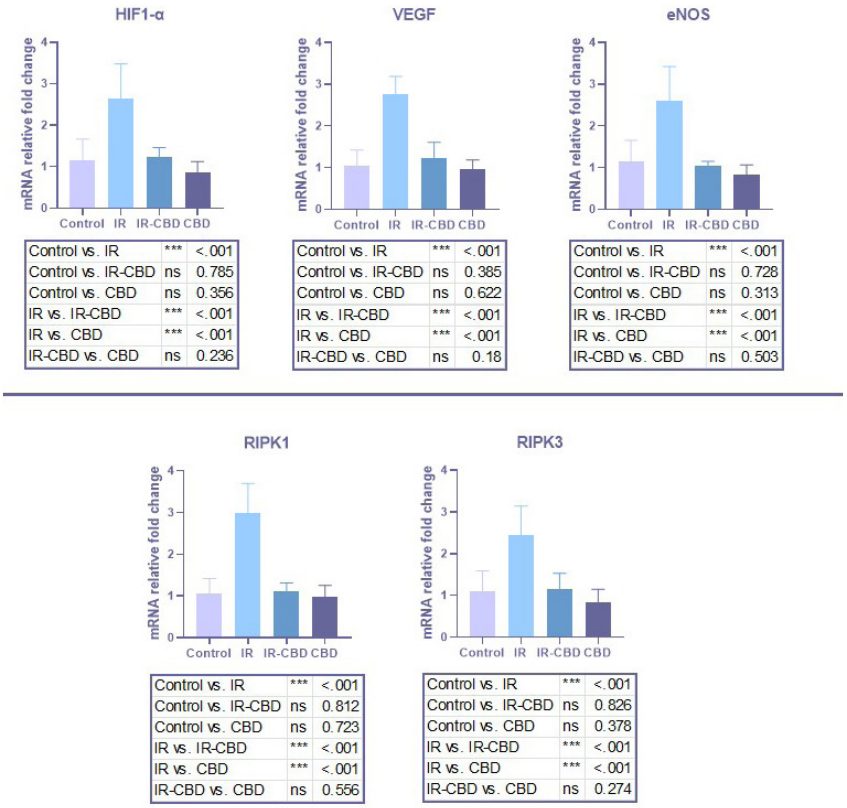

Control vs. IR	***	<.001
Control vs. IR-CBD	ns	0.785
Control vs. CBD	ns	0.356
IR vs. IR-CBD	***	<.001
IR vs. CBD	***	<.001
IR-CBD vs. CBD	ns	0.236

Control vs. IR	***	<.001
Control vs. IR-CBD	ns	0.385
Control vs. CBD	ns	0.622
IR vs. IR-CBD	***	<.001
IR vs. CBD	***	<.001
IR-CBD vs. CBD	ns	0.18

Control vs. IR	***	<.001
Control vs. IR-CBD	ns	0.728
Control vs. CBD	ns	0.313
IR vs. IR-CBD	***	<.001
IR vs. CBD	***	<.001
IR-CBD vs. CBD	ns	0.503

Control vs. IR	***	<.001
Control vs. IR-CBD	ns	0.812
Control vs. CBD	ns	0.723
IR vs. IR-CBD	***	<.001
IR vs. CBD	***	<.001
IR-CBD vs. CBD	ns	0.556

Control vs. IR	***	<.001
Control vs. IR-CBD	ns	0.826
Control vs. CBD	ns	0.378
IR vs. IR-CBD	***	<.001
IR vs. CBD	***	<.001
IR-CBD vs. CBD	ns	0.274

Figure 4. Relative mRNA expression in rat lung
IR: Ischemia/reperfusion; CBD: Cannabidiol; RIPK1: Receptor-interacting serine/threonine-protein kinase 1; RIPK3: Receptor-interacting serine/threonine-protein kinase 3; HIF-1α: Hypoxia-inducible factor-1 alpha; eNOS: Endothelial nitric oxide synthase; VEGF: Vascular endothelial growth factor. The criteria for statistical significance are **P*<0.05, ***P*<0.01, and ****P*<0.001.

Discussion

Reperfusion is defined as the restoration of blood flow after ischemia and is necessary to prevent further damage to an organ or tissue. However, the return of oxygen-enriched blood to areas that have experienced oxygen deprivation can cause more damage than that caused by ischemia alone (32). Tissue damage that occurs after ischemia due to platelet activation and ATP depletion can be further triggered by ROS production during reperfusion (33). ROS activates the oxidative stress mechanism, which is a condition caused by an imbalance between oxidants and anti-oxidants (4). Additionally, the lungs receiving a dual blood supply from both pulmonary and bronchial arteries and performing dual oxygen exchange via the blood-alveolar barrier are factors that increase the severity of IR damage in the lungs. As a result, ROS can lead to membrane disruption, endothelial damage, irreversible injury, and ultimately apoptosis and necrotic cell death (3, 33).

CBD has many different impacts, including anti-inflammatory, anti-oxidant, antipsychotic, cardioprotective, and vasodilatory effects (23). CBD can have direct and indirect effects on oxidative stress by modulating the levels and activities of oxidants and anti-oxidants (25). A study has shown that CBD protects lipids and proteins from oxidative damage by regulating oxidative stress levels (5). This study assessed CBD's possible protection against lung injury using an induced IR model.

Following IR, ROS levels increase and activate the oxidative stress mechanism (6). According to biochemical analysis, TAS levels went down in the IR group, whereas TOS and OSI levels elevated. These findings suggest the development of oxidative damage in the lungs. In contrast, improvements were observed in the CBD-IR group, along with a reduction in oxidative stress in the lungs. This suggests that CBD has both direct and indirect effects on oxidative stress.

IR causes changes in oxygen concentrations in cells, and HIF-1α plays an important role in response to these changes. Activation of HIF-1α during hypoxia regulates VEGF release (6). A study on glioma cells demonstrated that CBD inhibits HIF-1α and VEGF and exhibits antineoplastic and antiangiogenic properties (34). Additionally, it is known that HIF-1α increases eNOS expression (6). eNOS is a downstream effector of VEGF and contributes to vascular permeability, inflammation, and angiogenesis during IR (11, 35, 36). The role of NO in IR is dual: while low levels are protective, excessive NO contributes to oxidative stress and inflammation (37, 38). In this study, significant reductions in HIF-1α, VEGF, and eNOS parameters were observed following CBD treatment. This suggests that CBD reduces IR by inhibiting the HIF-1α/VEGF/eNOS signaling pathways. While our data do not definitively prove that eNOS reduction is solely VEGF-dependent, the parallel down-regulation aligns with the known HIF-1α/VEGF/eNOS axis in IR injury. Nevertheless, further studies are needed to determine whether CBD modulates eNOS directly or exclusively through the HIF-1α/VEGF pathway.

Inflammation causes irreversible damage and ultimately leads cells to apoptosis. In a study examining the role of CBD in apoptosis, it was observed that CBD treatment in rats with cerebral ischemia reduced cytochrome C release, and this reduction decreased Cas-3 expression, the final step in both intrinsic and extrinsic apoptosis pathways. This suggests that CBD may have anti-apoptotic and anti-oxidant effects (39). In a study examining liver IR injury, it was found that CBD treatment administered immediately after ischemia induction or 90 min after reperfusion successfully alleviated liver damage at the 6th hour of reperfusion (40). Additionally, another study demonstrated that CBD prevents inflammation and cytotoxicity by inhibiting the TLR4/NLRP3/caspase-1 signaling pathways (41). It has been demonstrated that CBD treatment significantly inhibits apoptosis in kidney cells resulting from IR. In this study, the reduction in Cas-3 expression in CBD-treated rats indicates that apoptosis was effectively prevented. Additionally, CBD may inhibit apoptosis by reducing ROS and TNF-α production (42). In this study as well, the decrease in Cas-3 expression following CBD treatment was effective in preventing apoptosis.

In this study, a decrease in RIPK1 and RIPK3 levels was observed in rats after CBD administration, and necrotic cell death was reduced by histopathological examination. These results indicate that CBD affects RIPK1- and RIPK3-mediated necrotic cell death pathways.

Conclusion

These findings suggest that CBD holds promise as a therapeutic agent for the treatment of IR-induced lung injury. However, our study used a single CBD dose and short-term follow-up, so it could not assess the dose-response relationship and long-term effects. In addition, the absence of a sham group made it difficult to distinguish the effects of surgical stress. Future studies aim to test different doses (1-10 mg/kg) and reperfusion times of 24–72 hr.

Acknowledgment

Financial support for this research was provided by the Scientific Research Fund of Suleyman Demirel University, with Project Number TSG-2023-9010.

Data Availability

The data for supporting the results of this research are available from the corresponding author upon reasonable request.

Ethics Approval and Consent to Participate

All experimental protocols were approved by Suleyman Demirel University's Local Ethical Committee on Animal Research (approval no: 26.01.2023-01-119) and followed the guidelines for animal research published in Animal Research: Reporting *In vivo* Experiments (ARRIVE) 2.0. The Scientific Projects Commission of the University of Suleyman Demirel University, under Project Number TSG-2023-9010, supplied the funding for this study.

Authors' Contributions

All authors conceived and designed the research. HE C, SE A, S Y, MA S, and M S performed experiments and collected data. I I, MY T, M S, and O O analyzed data. HE C, R Y, and O O supervised, directed, and managed the study. All authors wrote the manuscript and read and approved the final version to be published.

Conflicts of Interest

The authors declare that they have no competing interests.

Declaration

We acknowledge the use of GPT-5.1 to rephrase and reduce plagiarism while improving language and grammar.

References

1. Kandilci HB, Gümüşel B. Akciğerlerde İskemi-reperfüzyon hasarı ve İskemik önkoşullama. Hacettepe Univ J Fac Pharm 2005; 1:35–49.
2. Alaçam B, Ek RO, Yıldız Y, Serter M, Boylu NT, Temoçın S. The effect of carnosine on lung injury induced by abdominal aortic ischemia-reperfusion. Meandros Med Dent J 2010;11:41–47.
3. Tang H, Sun L, Huang J, Yang Z, Li C, Zhou X. The mechanism and biomarker function of Cavin-2 in lung ischemia-reperfusion injury. Comput Biol Med 2022;151:106234.
4. Kim EK, Jang M, Song MJ, Kim D, Kim Y, Jang HH. Redox-mediated mechanism of chemoresistance in cancer cells. Antioxidants 2019;8:471.
5. Atalay S, Jarocka-Karpowicz I, Skrzydlewska E. Antioxidative and anti-inflammatory properties of cannabidiol. Antioxidants 2019;9:21.
6. Zhang Z, Yao L, Yang J, Wang Z, Du G. PI3K/Akt and HIF-1 signaling pathway in hypoxia-ischemia. Mol Med Rep 2018;18:3547–3554.
7. Khosropoor S, Alavi MS, Etemad L, Roohbakhsh A. Cannabidiol goes nuclear: The role of PPARγ. Phytomedicine 2023;114:154771.
8. Liu C, Pei S, Dai H, Liu Z, Ye M, Liu H, *et al.* Downregulation of SIRT3 aggravates lung ischemia reperfusion injury by increasing mitochondrial fission and oxidative stress through HIF-1α-Dependent mechanisms. Oxid Med Cell Longev 2022;2022:9041914.
9. Zhou J, Schmid T, Brune B. Tumor necrosis factor-α causes accumulation of a ubiquitinated form of hypoxia inducible factor-1α through a nuclear factor-κB-dependent pathway. Mol Biol Cell 2003;14:2216–2225.
10. Syukri A, Hatta M, Amir M, Rohman MS, Mappangara I, Kaelan C, *et al.* Doxorubicin induced immune abnormalities and inflammatory responses via HMGB1, HIF1-α and VEGF pathway in progressive of cardiovascular damage. Ann Med Surg 2022;76:103501.
11. Qiu Y, Chen C, Zhang J, Chen M, Gong H, Gong L, *et al.* VEGF attenuates lung injury by inducing homing of CD133+ progenitors via VEGFR1. Biochem Biophys Res Commun 2019;511:650–657.
12. Savitskaya MA, Onishchenko GE. Mechanisms of apoptosis. Biochem 2015;80:1393–1405.
13. Coşkun G, Özgür H. Apoptoz ve nekrozun moleküler mekanizması. Arşiv Kaynak Tarama Derg 2011;20:145–158.
14. Wani AK, Akhtar N, Mir T ul G, Singh R, Jha PK, Mallik SK, *et al.* Targeting apoptotic pathway of cancer cells with phytochemicals and plant-based nanomaterials. Biomolecules 2023;13:194.
15. Obeng E. Apoptosis (programmed cell death) and its signals-A review. Brazilian J Biol 2020;81:1133–1143.
16. Delhalle S, Duvoix A, Schnekenburger M, Morceau F, Dicato M, Diederich M. An introduction to the molecular mechanisms of apoptosis. Ann N Y Acad Sci 2003;1010:1–8.
17. Mizumura K, Maruoka S, Gon Y, Choi AMK, Hashimoto S. The role of necroptosis in pulmonary diseases. Respir Investig 2016;54:407–412.
18. Shan B, Pan H, Najafov A, Yuan J. Necroptosis in development and diseases. Genes Dev. 2018;32:327–340.
19. Jun W, Benjanuwattra J, Chattipakorn SC, Chattipakorn N. Necroptosis in renal ischemia/reperfusion injury: a major mode of cell death? Arch Biochem Biophys 2020;689:108433.
20. Yu Z, Jiang N, Su W, Zhuo Y. Necroptosis: a novel pathway in neuroinflammation. Front Pharmacol 2021;12:701564.
21. Arruza L, Pazos MR, Mohammed N, Escribano N, Lafuente H, Santos M, *et al.* Cannabidiol reduces lung injury induced by hypoxic–ischemic brain damage in newborn piglets. Pediatr Res 2017;82:79–86.
22. Erdem S, Gonca E, Başoğlu G, Aydemir E. İskemi Sonrası Verilen Kannabidiol Reperfüzyon ile Uyarılan Aritmilere Karşı Koruyucu Etkilidir. Batı Karadeniz Tıp Derg 2022;6:16–23.
23. Kicman A, Toczek M. The effects of cannabidiol, a non-intoxicating compound of cannabis, on the cardiovascular system in health and disease. Int J Mol Sci 2020;21:6740.
24. Etemad L, Karimi G, Alavi MS, Roohbakhsh A. Pharmacological effects of cannabidiol by transient receptor potential channels. Life Sci 2022;300:120582.
25. Pereira SR, Hackett B, O'Driscoll DN, Sun MC, Downer EJ. Cannabidiol modulation of oxidative stress and signalling. Neuronal Signal 2021;5:NS20200080.
26. Abu-Amara M, Yang SY, Tapuria N, Fuller B, Davidson B, Seifalian A. Liver ischemia/reperfusion injury: Processes in inflammatory networks—a review. Liver Transplant 2010;16:1016–1032.
27. Akin SE, Asci H, Tepebasi MY, Ilhan İ, Ozmen Ö, Comlekci S, *et al.* Prophylactic effects of radiofrequency electromagnetic field on pulmonary ischemia-reperfusion via HIF-1α/eNOS pathway and BCL2/BAX signaling. Pulm Circ 2025;15:e70051.
28. İlhan İ, Ascı H, Buyukbayram Hİ, Imeci OB, Sevuk MA, Erol Z, *et al.* The impact of the high-fructose corn syrup on cardiac damage via SIRT1/PGC1-α pathway: Potential ameliorative effect of selenium. Biol Trace Elem Res 2024;202: 5166-5176.
29. Tveden-nyborg P, Lykkesfeldt J. BCPT 2023 policy for experimental and clinical studies. Basic Clin Pharmacol Toxicol 2023;133:391–396.
30. Ozmen O, Milletsever A, Tasan S, Selcuk E, Savran M. The effects of cannabidiol against Methotrexate-induced lung damage. Basic Clin Pharmacol Toxicol 2024;134:695–703.
31. Topsakal S, Ozmen O, Asci H, Gulal A, Ozcan KN, Aydin B. Dapagliflozin prevents reproductive damage caused by acute systemic inflammation through antioxidant, anti-inflammatory, and antiapoptotic mechanisms. Basic Clin Pharmacol Toxicol 2024;135:561–574.
32. Halladin NL. Oxidative and inflammatory biomarkers of ischemia and reperfusion injuries. Dan Med J 2015;62:B5054.
33. Akkoç H, Kelle İ, Kale E. Sıçan akciğerinde oluşturulan iskemik önkoşullamanın kalpteki iskemi reperfüzyon hasarı üzerine etkileri. Dicle Tıp Derg 2008;35:102–109.
34. Solinas M, Massi P, Cinquina V, Valenti M, Bolognini D, Gariboldi M, *et al.* Cannabidiol, a non-psychoactive cannabinoid compound, inhibits proliferation and invasion in U87-MG and T98G glioma cells through a multitarget effect. PLoS One 2013;8:e76918.
35. He H, Venema VJ, Gu X, Venema RC, Marrero MB, Caldwell RB. Vascular endothelial growth factor signals endothelial cell production of nitric oxide and prostacyclin through flk-1/KDR activation of c-Src. J Biol Chem 1999;274:25130–25135.
36. Fukumura D, Gohongi T, Kadambi A, Izumi Y, Ang J, Yun CO, *et al.* Predominant role of endothelial nitric oxide synthase in vascular endothelial growth factor-induced angiogenesis and vascular permeability. Proc Natl Acad Sci 2001;98:2604–2609.
37. Esposito G, De Filippis D, Maiuri MC, De Stefano D, Carnuccio R, Iuvone T. Cannabidiol inhibits inducible nitric oxide synthase protein expression and nitric oxide production in β-amyloid stimulated PC12 neurons through p38 MAP kinase and NF-κB involvement. Neurosci Lett 2006;399:91–95.
38. Lundberg JO, Weitzberg E. Nitric oxide signaling in health and disease. Cell 2022;185:2853–2878.
39. Khaksar S, Bigdeli M, Samiee A, Shirazi-Zand Z. Antioxidant and anti-apoptotic effects of cannabidiol in model of ischemic stroke in rats. Brain Res Bull 2022;180:118–130.
40. Mukhopadhyay P, Rajesh M, Horváth B, Bátkai S, Park O, Tanchian G, *et al.* Cannabidiol protects against hepatic ischemia/reperfusion injury by attenuating inflammatory signaling and response, oxidative/nitrative stress, and cell death. Free Radic Biol Med 2011;50:1368–1381.
41. Corpetti C, Del Re A, Seguella L, Palenca I, Rurgo S, De Conno B, *et al.* Cannabidiol inhibits SARS-Cov-2 spike (S) protein-induced cytotoxicity and inflammation through a PPARγ-dependent

TLR4/NLRP3/Caspase-1 signaling suppression in Caco-2 cell line. Phyther Res 2021;35:6893–6903.
42. Fouad AA, Al-Mulhim AS, Jresat I. Cannabidiol treatment ameliorates ischemia/reperfusion renal injury in rats. Life Sci 2012;91:284–292.